

# Direct Analysis of Water Content and Movement in Single Dormant Bacterial Spores Using Confocal Raman Microspectroscopy and Raman Imaging

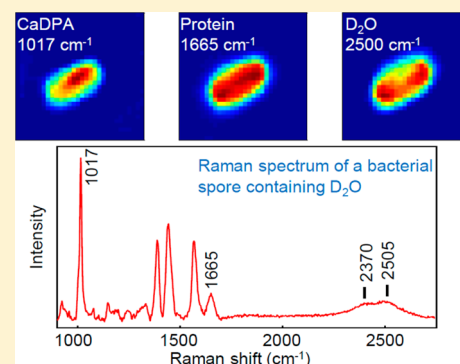
Lingbo Kong,<sup>†</sup> Peter Setlow,<sup>‡</sup> and Yong-qing Li<sup>\*†</sup>

<sup>†</sup>Department of Physics, East Carolina University, Greenville, North Carolina 27858-4353, United States

<sup>‡</sup>Department of Molecular, Microbial and Structural Biology, University of Connecticut Health Center, Farmington, Connecticut 06030-3305, United States

## S Supporting Information

**ABSTRACT:** Heavy water (D<sub>2</sub>O) has a distinct molecular vibration spectrum, and this has been used to analyze the water content, distribution, and movement in single dormant *Bacillus cereus* spores using confocal Raman microspectroscopy and Raman imaging. These methods have been used to measure the kinetics of D<sub>2</sub>O release from spores suspended in H<sub>2</sub>O, the spatial distribution of D<sub>2</sub>O in spores, and the kinetics of D<sub>2</sub>O release from spores during dehydration in air at room temperature. The results obtained were as follows. (1) The Raman spectrum of single D<sub>2</sub>O-loaded dormant spores suggests that D<sub>2</sub>O in spores is in a relatively weak hydrogen-bonded mode, compared to the strong hydrogen-bonded mode in pure D<sub>2</sub>O. (2) The D<sub>2</sub>O content of individual spores in a population was somewhat heterogeneous. (3) The spatial distribution of D<sub>2</sub>O in single dormant spores is uneven, and is less dense in the central core region. Raman images of different molecular components indicate that the water distribution is somewhat different from those of proteins and Ca-dipicolinic acid. (4) Exchange of spore D<sub>2</sub>O with external H<sub>2</sub>O took place in less than 1 s. (5) However, release of spore D<sub>2</sub>O during air dehydration at room temperature was slow and heterogeneous and took 2–3 h for complete D<sub>2</sub>O release.



When starved, bacteria of various *Bacillus* species can form endospores that can survive in a metabolically dormant state for many years.<sup>1,2</sup> These dormant spores are also very resistant to a variety of harsh conditions.<sup>3,4</sup> The remarkably low water content in the central spore core, 25–50% of wet weight depending on the species, is believed to be a major factor in spores' dormancy and resistance.<sup>5</sup> Consequently, studies of the properties and dynamics of water in spores, in particular core water, are important for understanding the mechanisms leading to spores' remarkable properties. A number of studies have demonstrated that dormant spores are permeable to water and that water in spores has high mobility.<sup>6–16</sup> Indeed, water can diffuse between the spore core and the environment, as using deuterated water (D<sub>2</sub>O), > 97% of the water in spores was found to exchange with the environment.<sup>10</sup> Similarly, a nuclear magnetic relaxation technique measured the speed of water permeation into the spore core or external water exchange with water contained within the spore as on a time scale of <1 min.<sup>16</sup> Dipicolinic acid (DPA) comprises a large amount (10–20%) of the dry weight of bacterial spores and is located in the spore's central core as a 1:1 chelate with divalent cations, predominantly Ca<sup>2+</sup> (CaDPA); this latter compound plays a key role in reducing the spore core water content.<sup>17–21</sup> CaDPA has been demonstrated to have minimal if any mobility in hydrated dormant spores,<sup>13</sup> and at least one normally freely mobile spore core protein is also immobilized.<sup>22</sup> Given the

relatively high mobility of water in the spore core, spore dormancy has been suggested to be due to dehydration-induced conformational changes in key enzymes.<sup>16</sup>

Although water in bacterial spores and water permeability of spores has been extensively studied,<sup>6–16,23,24</sup> most of these studies were performed on spore populations. However, direct information on water content and permeability in individual spores under physiological conditions is still limited. A deeper understanding of spore properties can often be obtained by analysis of the behavior of individual spores. Raman spectroscopy is a powerful technique for noninvasive molecular analysis of living cells and has been used to analyze various molecular components in and the dynamics of single bacterial spores.<sup>26–32</sup> Using this technique, we have recently characterized the amount of water surrounding CaDPA molecules in spores by measuring changes in CaDPA Raman bands in the core of single spores exposed to hydrated and dehydrated environments.<sup>33</sup> High-resolution secondary ion mass spectrometry (nano-SIMS) has also been used to spatially characterize water and ion incorporation in individual bacterial spores and to obtain images of D<sub>2</sub>O and ions taken up by single spores.<sup>25</sup>

Received: February 18, 2013

Accepted: July 2, 2013

Published: July 2, 2013

However, the spore samples had to be placed in an ultrahigh vacuum (UHV) in order to do the nano-SIMS analysis, and this vacuum removed the majority of unbound water, caused spore damage, and precluded direct analysis under spores' normal physiological condition. In addition, this study did not provide information on water distribution relative to that of other intrinsic spore molecules, nor any kinetic analyses of water movement into and out of spores.

In this paper, we have used Raman microspectroscopy and multifocus Raman imaging techniques to study D<sub>2</sub>O water content, spatial distribution, and movement in individual dormant *Bacillus cereus* spores. Comparison of the D<sub>2</sub>O Raman band of individual D<sub>2</sub>O-loaded spores with that of pure D<sub>2</sub>O indicates that the state of water in dormant spores is different from that of pure water. Quantitative analysis of Raman spectra of single D<sub>2</sub>O-loaded spores also enabled measurement of the weight of D<sub>2</sub>O in single dormant spores. Raman images of CaDPA, protein, and D<sub>2</sub>O bands in single dormant *B. cereus* spores were measured simultaneously to reveal the relative spatial distribution of these molecules inside spores. Finally, the kinetics of exchange of external H<sub>2</sub>O with spore D<sub>2</sub>O and the loss of D<sub>2</sub>O during air-drying of single dormant spores were investigated by analysis of Raman images and spectral intensity. The advantages of these analytical methods include (1) the spores can be noninvasively analyzed in their native environment at room temperature,<sup>32,33</sup> (2) the time scale of Raman spectroscopic analysis can be decreased to ~1 s,<sup>30</sup> (3) multiple individual spores can be analyzed simultaneously in one experiment,<sup>34</sup> and multiple molecular components can be analyzed simultaneously by spontaneous Raman imaging.<sup>31</sup>

## METHODS

**Bacterial Strain and Spore Preparation.** The *Bacillus* species used in this work is *B. cereus* T (originally obtained from H.O. Halvorson). Spores were prepared at 30 °C in liquid defined sporulation medium, harvested by centrifugation, purified, and stored in water (H<sub>2</sub>O) at 4 °C, as described previously.<sup>35</sup> Purified spores were free (>98%) of vegetative or sporulating cells, cell debris, and germinated spores, as observed by phase contrast microscopy.

**Removal of H<sub>2</sub>O from Spores and D<sub>2</sub>O Uptake.** Spores suspended in H<sub>2</sub>O were dehydrated, using low-vacuum drying.<sup>33</sup> A drop of spore suspension (1 μL) was placed on a quartz coverslip. The coverslip was placed in a small vacuum chamber with a vacuum pressure of 1.0 Pa for more than 3 h under continuous pumping. After removal of H<sub>2</sub>O, 20 μL D<sub>2</sub>O liquid (Acros Organics, 99.8 atom % D) was added over the spores on the coverslip, and the coverslip was incubated for >30 min at room temperature to allow D<sub>2</sub>O uptake. Spores incubated in this manner in liquid D<sub>2</sub>O were kept at 4 °C for several days.

**Confocal Raman microspectroscopy and multifocus Raman imaging.** Raman microspectroscopy was carried out using a multifocus confocal Raman system constructed on an external phase contrast microscope.<sup>31,32,34</sup> A near-infrared high-power external cavity diode laser at 780 nm (Sacher Lasertechnik, TEC-300-0780-0500) served as the Raman excitation source. The laser source had a frequency bandwidth <1 MHz with the wavelength stabilized (<0.1 nm). An objective with high numerical aperture (Plan Apo 60×, NA = 1.4) equipped on an inverted microscope (Ti-S, Nikon) was used to focus the laser beam. A 50 μm confocal pinhole was

used in the Raman optical route giving a diffraction limited resolution of 0.46 and 1.2 μm in the lateral and axial directions, respectively.<sup>31</sup> This limited spatial resolution would affect the analysis for small *B. cereus* spores of ~1.5 μm in average size (see Discussion). Phase contrast microscopy allows the selection of dormant spores that appear phase bright. Raman spectra were collected with WINSPEC/32 software and spectral data analysis was carried out with MATLAB code. A pair of galvo mirrors (Cambridge Technology, 6220H) were used to steer the incident laser beam for multifocus scans and Raman image scans. Another galvo mirror (GVS001, Thorlabs Inc.) in front of the spectrograph (LS-785, Princeton Instruments) synchronously steered the backward Raman scattering light from each focus point onto different vertical positions of a multichannel CCD detector (PIXIS 400BR, Princeton Instruments). This multifocus confocal Raman microspectroscopy system allows parallel measurements on multiple individual bacterial spores in random positions on a quartz coverslip.<sup>34</sup> Raman image measurement was also based on this multifocus confocal Raman system.<sup>31</sup> Raman images of individual spores were obtained by scanning a one-dimension foci array (30 foci) across the specimen, and the Raman spectra of all 30 foci could be collected simultaneously. In this paper, a single spore was covered by a total of 30 × 30 foci generating a Raman image of 30 × 30 pixels with a step size of 127 nm per pixel. The typical time-averaged laser power was 2.5 mW per focus at 780 nm.

**Quantitative Analysis of D<sub>2</sub>O Raman Signal in Single Spores.** The laser focus was scanned by a pair of galvo mirrors at a frequency of 500 Hz to form a small square laser spot with an area of 2.5 × 2.5 μm<sup>2</sup> on a quartz coverslip. Before Raman measurements on D<sub>2</sub>O-loaded spores adhered on the quartz coverslip prepared as described below, residual liquid D<sub>2</sub>O was removed by a micropipet leaving a thin film of D<sub>2</sub>O–spore mixture on the surface of the coverslip. After exposure to air, the thin film of liquid D<sub>2</sub>O disappeared in a few min. Under phase contrast microscopy, images of spores with no surrounding liquid D<sub>2</sub>O look much brighter than spores surrounded by liquid D<sub>2</sub>O due to the difference in the index of refraction. The absence of liquid D<sub>2</sub>O around spores was also confirmed by Raman measurements; as for every spore examined in addition to each spore's Raman spectrum, a background spectrum from an adjacent spore-free area (2–3 μm away from the spore) on the coverslip was also measured. Checking the background's Raman spectrum ensured that all the liquid D<sub>2</sub>O around spores was gone. After spores were adhered on the coverslip and no residual liquid D<sub>2</sub>O remained, a phase contrast image of a spore was recorded by a digital camera and analyzed with the Matlab program to locate the central position of the spore. The 2.5 × 2.5 μm<sup>2</sup> laser scanning area was then guided by the galvo mirrors through the Matlab program to cover the single spore for measurement of Raman spectra.

Polystyrene beads of 1 μm in diameter (Bangs Laboratories Inc., with a standard deviation of 0.02 μm) were deposited on the surface of a quartz coverslip and mixed with pure D<sub>2</sub>O. The Raman spectrum of D<sub>2</sub>O with no polystyrene beads in the square laser scanning area was measured first. A second Raman spectrum was also measured with two closely adjacent polystyrene beads covered by the square laser scanning area. Subtracting the second Raman spectrum from the first gives the difference in the intensity of the D<sub>2</sub>O Raman band (between 2200 and 2700 cm<sup>-1</sup>, Figure 1), resulting from D<sub>2</sub>O displaced

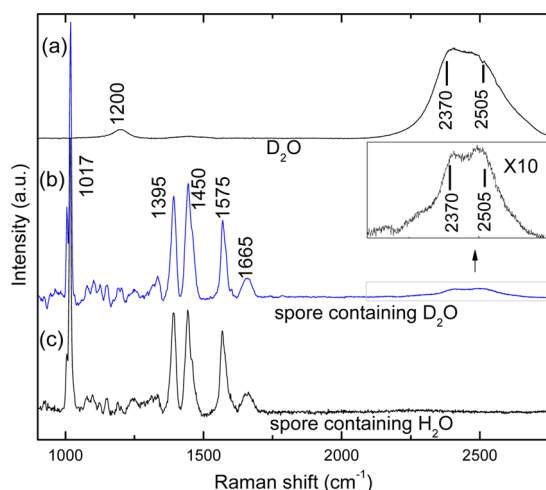


**Figure 1.** Raman spectra of (a) pure  $D_2O$ , (b) single dormant  $D_2O$ -loaded *B. cereus* spores, and (c) single dormant  $H_2O$ -loaded *B. cereus* spores. The Raman spectra of single spores with  $D_2O$  or  $H_2O$  were averaged over 20 individual dormant spores. The insert in (b) is the magnified view of the  $D_2O$  bands in the  $\sim 2500\text{ cm}^{-1}$  region. The intensities of the CaDPA band at  $1017\text{ cm}^{-1}$  were normalized to the same level in the spectra of single spores.

by the polystyrene beads. This number was then used to quantify weights of  $D_2O$  from measured  $D_2O$  Raman spectral intensities (Supporting Information).

**Raman Measurement of Kinetics of  $D_2O$ – $H_2O$  Exchange in Spores.** The laser focus was scanned by a pair of galvo mirrors at a frequency of 500 Hz to form a small square laser spot with an area of  $1 \times 1\ \mu\text{m}^2$  on the quartz coverslip. A thin film of a spore– $D_2O$  mixture (spores were prepared with full  $D_2O$  uptake) was placed on the quartz coverslip. After spores were adhered on the coverslip and no residual liquid  $D_2O$  remained as observed by phase contrast microscopy, a phase contrast image of one single spore was recorded by a digital camera and analyzed with the Matlab program to locate the central position of the spore. The  $1 \times 1\ \mu\text{m}^2$  laser scanning area was then guided by the galvo mirrors through the Matlab program to cover the single spore for a continuous measurement of Raman spectra with a time resolution of 1 s. To initiate the Raman measurements,  $40\ \mu\text{L}$  distilled  $H_2O$  was added to the sample holder by a micropipet, and all the spores attached on the coverslip were immediately exposed to the liquid  $H_2O$ . The  $D_2O$  level in the measured spores before and after adding  $H_2O$  was calculated from the recorded Raman spectra.

**Real-Time Raman Measurements of Loss of  $D_2O$  from Single Spores during Air-Drying.** A  $D_2O$ -spore mixture on a quartz coverslip was air-dried at room temperature as described above until residual liquid  $D_2O$  had disappeared around the spores as observed by phase contrast microscopy; this time was defined as 0 min and the Raman measurement began. Raman spectra of 5–10 single spores were measured simultaneously<sup>34</sup> with a time resolution of 30 s, or the Raman image of one spore was acquired with 10 min per frame. Five to ten single spores were continuously monitored by Raman spectroscopy, or a single spore was monitored by Raman imaging for 3 h. For long Raman measurements, an active locking system was used to lock the distance between the piezo-driven objective and the spore sample to stabilize the focusing drift in the  $Z$  direction. The long-term stability of the locking along the  $Z$  direction was  $\sim 10\text{ nm}$ , and the autolocking could

last for more than 12 h.<sup>33</sup> An image analysis program was developed to analyze the phase contrast image to allow relocating of the center positions of spores under study to compensate for any drifts in the  $xy$  directions due to horizontal position changes of the spore sample holder.<sup>33</sup> These efforts in controlling microscope stability enabled us to successfully measure the Raman signal from the  $1\text{--}2\ \mu\text{m}$  single spores for several hours. The average error of measured Raman band intensity was  $\sim 5\%$  in our Raman system.

**Data Analysis.** A custom-built Matlab program was used to analyze the Raman spectral data. For each single spore that was attached on the quartz coverslip, its Raman spectrum was measured and a background Raman spectrum was also measured at an empty region of the quartz coverslip ( $\sim 3\ \mu\text{m}$  away from the target spore) (see Figure S1 of the Supporting Information). Standard data processing procedures were used to obtain a single spore's Raman spectrum (such as Figures 1, 4b and 6a): (1) the background spectrum was subtracted from spore's raw Raman spectrum, (2) the subtracted spectrum was then smoothed using the Savitzky–Golay filter method, (3) a baseline was generated and subtracted to obtain a single spore's Raman spectrum (Figure S2 of the Supporting Information). From the processed spectrum of a single *B. cereus* spore containing  $D_2O$  (Figure 1c), a very clean spectral feature in  $2000\text{ cm}^{-1}$  and  $2800\text{ cm}^{-1}$  was shown, which was the Raman O–D stretch band of  $D_2O$ .

For quantitative evaluation of  $D_2O$  levels in single spores, we calculated the intensity values of the O–D band between  $2200$  and  $2700\text{ cm}^{-1}$  as follows: (1) the raw spore's spectrum was background-removed and smoothed as stated above, (2) the average baseline value was calculated by averaging all intensity values from  $2000$  to  $2200\text{ cm}^{-1}$  and from  $2700$  to  $2740\text{ cm}^{-1}$ , (3) the intensity values between  $2200$  and  $2700\text{ cm}^{-1}$  were summed and the average baseline value was subtracted to obtain the summed intensity value of the O–D band from single spores.

Another custom-built Matlab program was used to generate the Raman image ( $30 \times 30$  pixels). For each single spore attached on the quartz coverslip, Raman spectra at  $30 \times 30$  foci that cover the spore were acquired. The background Raman spectra were also acquired at a region of the same size with no spore, and these background spectra were identical for a quartz coverslip. The first step of the data processing was to get the averaged background spectrum by averaging the measured background spectra. The second step was to subtract the averaged background spectrum from each of the  $30 \times 30$  Raman spectra. The third step was to reduce the noise of the Raman image data set by using the singular value decomposition (SVD) method. The intensities of selected Raman bands were then calculated to form the Raman image.

## RESULTS

**Raman Spectra of Pure  $D_2O$  and Single Dormant Spores with  $H_2O$  or  $D_2O$ .** The Raman spectrum of pure  $D_2O$  is shown in Figure 1a. The band at  $1200\text{ cm}^{-1}$  is assigned to a D–O–D bend, and a broad envelope band around  $2500\text{ cm}^{-1}$  (between  $2200$  and  $2700\text{ cm}^{-1}$ ) is assigned to an O–D stretch.<sup>36,37</sup> The O–D stretch vibration is very sensitive to hydrogen-bonding and can be decomposed into four modes:<sup>37</sup> the peak at  $2370\text{ cm}^{-1}$  is assigned to the  $\nu_s(\text{O–D})$  of water in a strongly hydrogen-bonded environment called the icelike mode, the peak at  $2505\text{ cm}^{-1}$  is assigned to symmetrically and asymmetrically hydrogen-bonded water [ $\nu_s(\text{O–D})$  and



$\nu_{as}(\text{O-D})$ ] that is often called the liquidlike mode, and two peaks at 2607 and 2675  $\text{cm}^{-1}$  are assigned to weakly hydrogen-bonded modes which do not contribute significantly to the network structure of water.<sup>37</sup> Figure 1a shows that the peaks at 2370 and 2505  $\text{cm}^{-1}$  are dominant, indicating the strong hydrogen-bonded environment in pure  $\text{D}_2\text{O}$ . Figure 1c shows the Raman spectrum of a single dormant *B. cereus* spores containing  $\text{H}_2\text{O}$  with notable bands at 1017, 1395, and 1575  $\text{cm}^{-1}$  that are assigned to CaDPA's symmetric ring "breathing", the O-C-O symmetric stretch and ring stretch, respectively.<sup>33,38</sup> Another notable band at 1445  $\text{cm}^{-1}$  includes contributions from CaDPA as well as from spore proteins and lipids, and the band at 1665  $\text{cm}^{-1}$  corresponds to protein amide I.<sup>39</sup> Figure 1b shows the average Raman spectrum of single  $\text{D}_2\text{O}$ -loaded dormant *B. cereus* spores that contain the same CaDPA bands, as well as a predominant O-D stretch band of  $\text{D}_2\text{O}$  at  $\sim 2500$   $\text{cm}^{-1}$ , which does not appear in the spectrum of a spore with  $\text{H}_2\text{O}$  (Figure 1c). The clean Raman spectral feature of the O-D stretch band at  $\sim 2500$   $\text{cm}^{-1}$  allowed a good quantitative analysis of  $\text{D}_2\text{O}$  in single spores. The Raman spectra in Figure 1b were measured for the spores containing  $\text{D}_2\text{O}$  attached on the quartz coverslide when no liquid  $\text{D}_2\text{O}$  is surrounding them. Note that background spectra from an empty area of the quartz coverslip near the target spores had been subtracted, and thus the great majority of the  $\text{D}_2\text{O}$  seen in such spectra of single spores is actually in the spores (Supporting Information).

The details of the Raman spectrum of the  $\text{D}_2\text{O}$  bands in the 2500  $\text{cm}^{-1}$  region in single dormant spores containing  $\text{D}_2\text{O}$  (Figure 1a) are slightly different from those in pure  $\text{D}_2\text{O}$  (Figure 1b). The peak at 2505  $\text{cm}^{-1}$  showed a higher intensity, and the peak at 2370  $\text{cm}^{-1}$  [ $\nu_s(\text{O-D})$  mode in a strong hydrogen-bonded environment] showed a lower intensity in the spores containing  $\text{D}_2\text{O}$  (Figure 1b). These differences indicate that the strong hydrogen-bonded environment in pure  $\text{D}_2\text{O}$  has been weakened for the  $\text{D}_2\text{O}$  in bacterial spores. This suggests that  $\text{D}_2\text{O}$  in dormant spores is not in a bulk water environment and demonstrates that the state of  $\text{D}_2\text{O}$  in dormant bacterial spores is different from that in pure liquid  $\text{D}_2\text{O}$ .

#### Weight of $\text{D}_2\text{O}$ in Single Dormant *B. cereus* Spores.

The average weight of  $\text{D}_2\text{O}$  in a single dormant *B. cereus* spores was measured by quantitative analysis of Raman spectra. Spores were first dehydrated by vacuum drying to fully remove  $\text{H}_2\text{O}$ , then exposed to pure  $\text{D}_2\text{O}$ , briefly air-dried to remove liquid  $\text{D}_2\text{O}$ , and the Raman spectra of multiple single spores were measured in  $\sim 1$  min after the removal of the surrounding  $\text{D}_2\text{O}$ . This short measurement time should minimize loss of  $\text{D}_2\text{O}$  from within spores. The intensity of the  $\text{D}_2\text{O}$  Raman band between 2200 and 2700  $\text{cm}^{-1}$  was then used to calculate the weight of  $\text{D}_2\text{O}$  in each individual spore (Figure 2). The average weight of  $\text{D}_2\text{O}$  in a single dormant *B. cereus* spore was  $4.8 \times 10^{-13}$  g with a standard deviation of 18% (a minimum weight of  $3.2 \times 10^{-13}$  g and a maximum weight of  $6.1 \times 10^{-13}$  g).

**Raman images of  $\text{D}_2\text{O}$ , CaDPA, and Protein in Single Dormant *B. cereus* Spores.** Phase-contrast images and Raman images of two single dormant *B. cereus* spores with  $\text{D}_2\text{O}$  are shown in Figure 3 (panels a and b, respectively). The outer edges of ellipses from phase-contrast images were used as a reference to show the spore's outer edge in their Raman images. Since CaDPA is only in the spore core while proteins are found throughout the spore, the size of the CaDPA Raman images (Figure 3, panels a2 and b2) is slightly smaller than the

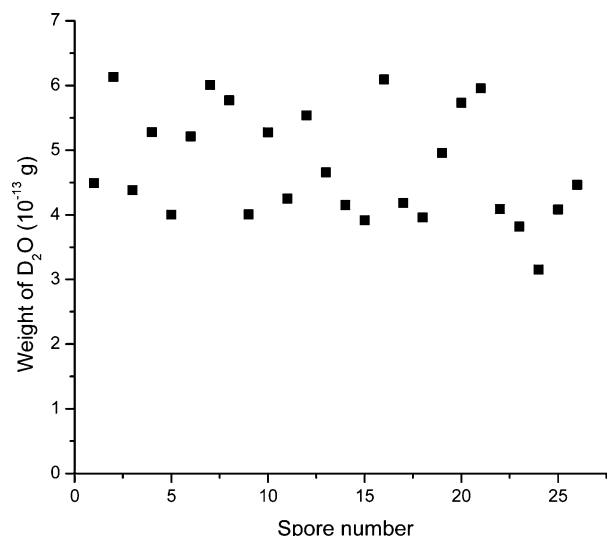


**Figure 2.** Measured weight of  $\text{D}_2\text{O}$  in 26 individual dormant *B. cereus* spores.

size of protein Raman images (Figure 3, panels a3 and b3).  $\text{D}_2\text{O}$  Raman images (Figure 3, panels a4 and b4) have almost the same size as protein Raman images, which suggests that  $\text{D}_2\text{O}$  distributes throughout the whole spore. In contrast to the CaDPA and protein Raman images showing a high concentration in the core or an even distribution, respectively, the  $\text{D}_2\text{O}$  Raman image showed a high concentration at the edge of the spore core, and a very low  $\text{D}_2\text{O}$  concentration in the core where there is the highest concentration of CaDPA. This pattern of  $\text{D}_2\text{O}$  distribution throughout the spore is the first direct measurement of water distribution in spores, and the results are consistent with indirect assessments of  $\text{H}_2\text{O}$  distribution in spores.<sup>1</sup>

#### Kinetics of Exchange of External $\text{H}_2\text{O}$ with $\text{D}_2\text{O}$ within the Spore.

Single  $\text{D}_2\text{O}$ -loaded dormant *B. cereus* spores were also used to measure  $\text{D}_2\text{O}$  exchange with external  $\text{H}_2\text{O}$ . Figure 4 (panels a and b) show the kinetics of the change in  $\text{D}_2\text{O}$  level and sequential Raman spectra, respectively, of a single  $\text{D}_2\text{O}$ -loaded dormant spore before and after the addition of liquid  $\text{H}_2\text{O}$ . Before the addition of liquid  $\text{H}_2\text{O}$ , Raman spectra of the single spore were acquired sequentially with a time interval of 1 s, showing that the spore initially contained  $\text{D}_2\text{O}$  molecules. After the addition of liquid  $\text{H}_2\text{O}$ , the spore was immediately exposed to and exchanged with liquid  $\text{H}_2\text{O}$  while its Raman spectra were measured continuously. The results from measurements on 5–10 individual spores indicate that all  $\text{D}_2\text{O}$  in the dormant spore exchanges rapidly with external  $\text{H}_2\text{O}$ , with a time scale for full water exchange of 1–2 s. Note that the time resolution of our Raman measurements was 1 s, so the timing difference between individual spores was limited by this time resolution. The actual exchange of spore  $\text{D}_2\text{O}$  with external  $\text{H}_2\text{O}$  took place in less than 1 s in individual spores.

#### Raman Analysis of Loss of $\text{D}_2\text{O}$ by Single Dormant *B. cereus* Spores during Air-Drying.

The air-drying of single  $\text{D}_2\text{O}$  loaded dormant *B. cereus* spores was also studied using Raman image analysis at room temperature. At 0 min, the size of the  $\text{D}_2\text{O}$  image was slightly larger than the size of the CaDPA image (Figure 5, panels a1 and b1), indicating that the  $\text{D}_2\text{O}$  molecules initially distributed both inside and outside the spore core. After 30 min of air drying, a comparison of Figure 5 (panels a2 or c2) with Figure 5 (panels a1 or c1) indicated

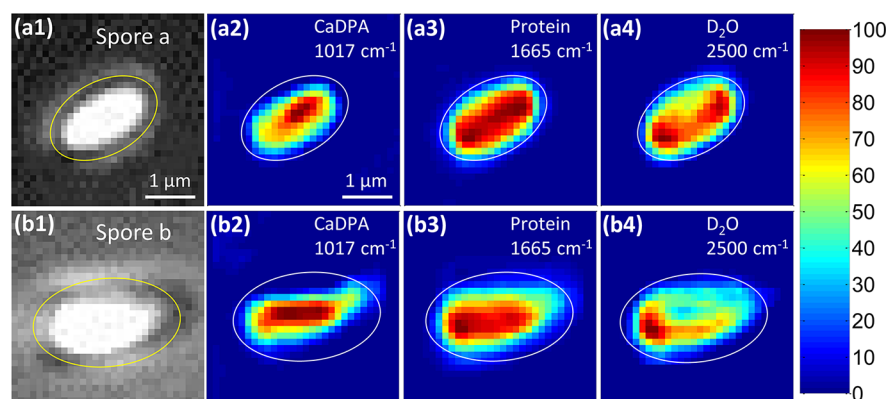


**Figure 3.** Phase-contrast images (a1 and b1) and Raman images (a2–a4 and b2–b4) of two individual dormant  $D_2O$ -loaded *B. cereus* spores. The ellipses in the phase-contrast images (a1 and b1) were used as a reference to mark the outer edge of the corresponding spores in Raman images (a2–a4) and (b2–b4).

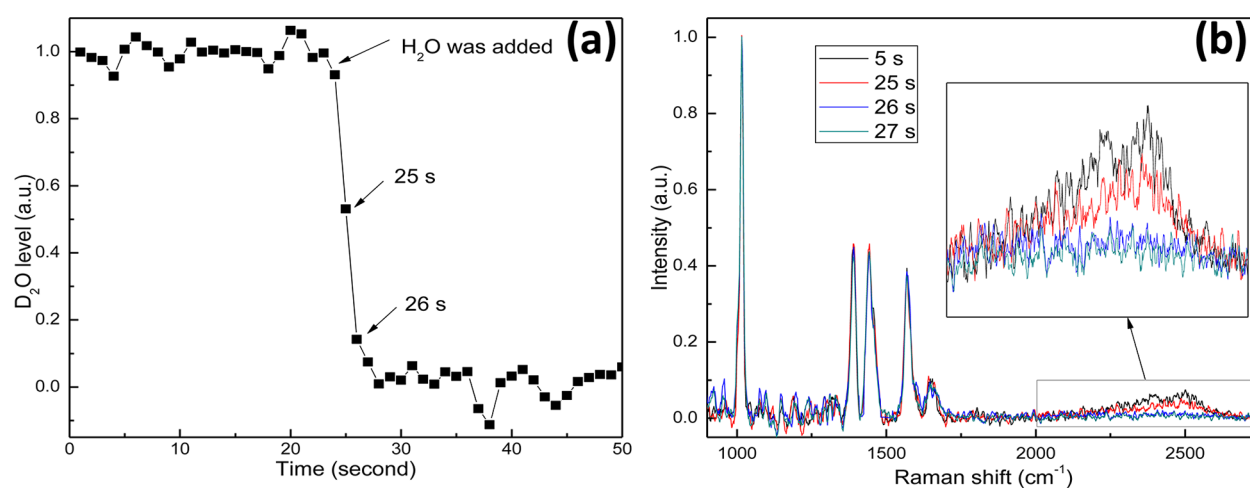


**Figure 4.** (a)  $D_2O$  level in a single *B. cereus* spore before and after addition of  $H_2O$  and (b) Raman spectra at 5, 25, 26, and 27 s of the single spore. The spore was initially  $D_2O$ -loaded.  $H_2O$  was added to the spores at the 23rd s, while the Raman spectra were acquired from the first second and, subsequently, every second with an acquisition time of 1 s. The inset in (b) is the expanded view of the  $D_2O$  bands at  $2500\text{ cm}^{-1}$ .

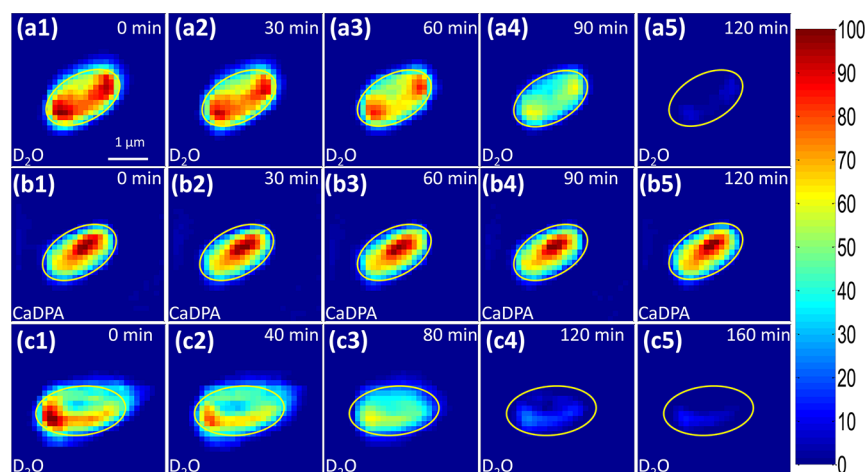


**Figure 5.** Raman images of the  $D_2O$  band at  $2500\text{ cm}^{-1}$  (a1–a5) and the CaDPA band at  $1017\text{ cm}^{-1}$  (b1–b5) of a single dormant *B. cereus* spore at various times during air-drying at room temperature. (c1–c5) shows the Raman images of the  $D_2O$  band at  $2500\text{ cm}^{-1}$  of another individual spore (with a larger size) during air drying. Ellipses in (a1–a5) and (b1–b5) are the same size and outline the outer edge of CaDPA Raman images of this spore. Ellipses in (c) are the same size and outline the outer edge of the CaDPA Raman image of spore b in Figure 3b2.

there was only an  $\sim 10\%$  decrease in total spore  $D_2O$  and no reduction in the area of  $D_2O$  distribution. After 1 h (Figure 5a3), the total  $D_2O$  level decreased by  $\sim 20\%$ , as calculated

from the corresponding  $D_2O$  Raman images, and the area with  $D_2O$  had decreased slightly in size. After 80–90 min (Figure 5, panels a4 and c3), the total  $D_2O$  level had decreased by  $\sim 45\%$ ,

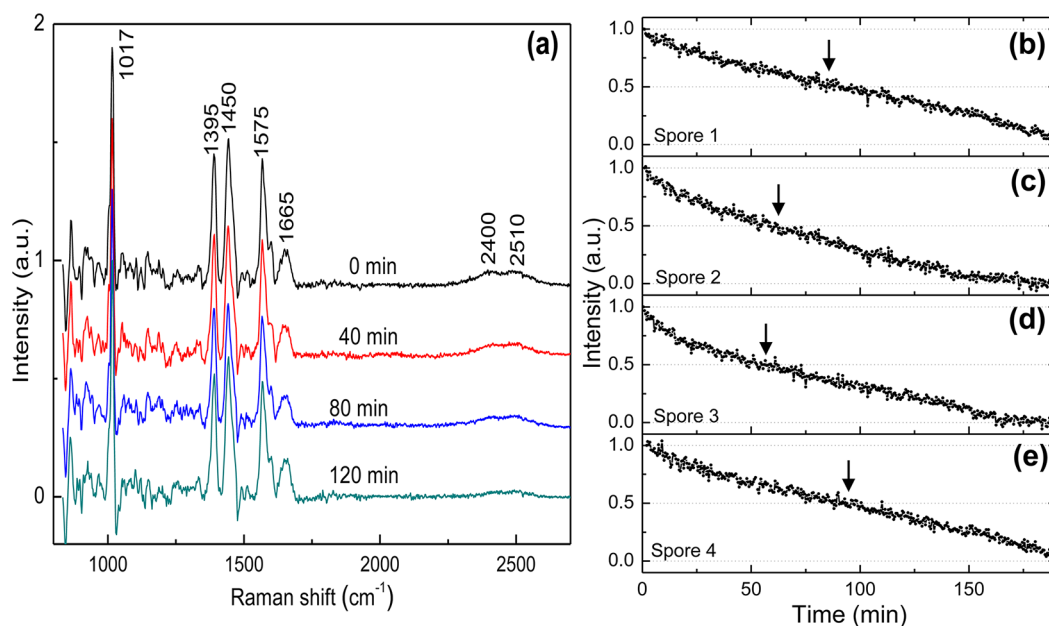


**Figure 6.** (a) Time-lapse Raman spectra of a single D<sub>2</sub>O-loaded *B. cereus* spore during air drying at room temperature. (b–e) Changes in levels of D<sub>2</sub>O in four individual spores as a function of time during air drying. The arrows indicate the times at which the D<sub>2</sub>O level drops to 50% of its initial value.

and D<sub>2</sub>O was found only in the core with the CaDPA. Note that the ellipses in Figure 5 (panels a and b) were from the outline of the CaDPA Raman images and were used to help in comparing CaDPA and D<sub>2</sub>O images. After 2 h of air-drying, less than 10% of the initial D<sub>2</sub>O remained in the spore core (Figure 5 (panels a5, c4, and c5)). In contrast to the dramatic changes in D<sub>2</sub>O distribution and level during air drying, the time-lapse Raman images of CaDPA in single spores (Figure 4b) showed no changes in the intensity and distribution of CaDPA over 2 h.

Figure 6a shows sequential Raman spectra of a single dormant D<sub>2</sub>O-loaded *B. cereus* spore during air drying, and Figure 6 (panels b–e) shows the intensity changes in total spore D<sub>2</sub>O as determined from Raman spectra as a function of the air-drying time for four individual single spores. The latter curves show slightly faster D<sub>2</sub>O loss in the first 30–40 min and then a subsequent more linear rate of loss. For some spores (Figure 6, panels c and d), no D<sub>2</sub>O could be detected by Raman spectroscopy after 150 min of air drying, while other spores exhibited a longer slow decrease in D<sub>2</sub>O for up to 3 h (Figure 6, panels b and e). Note that the time at which the D<sub>2</sub>O level dropped to 50% of its initial value was different for individual spores in the experiment, indicating that some individual spores dehydrated slightly faster and some slower in air at room temperature.

## DISCUSSION

The analysis of D<sub>2</sub>O in single dormant bacterial spores by confocal Raman microspectroscopy and Raman imaging has led to a better understanding of a number of aspects of the state, distribution, and mobility of water in spores. First, the D<sub>2</sub>O Raman spectrum in bacterial spores is different from that of pure D<sub>2</sub>O. This difference appears primarily as a decrease in the intensity of the Raman band at 2370 cm<sup>-1</sup> from strong hydrogen-bonded modes of D<sub>2</sub>O, while the intensity of the 2505 cm<sup>-1</sup> band due to relatively weak hydrogen-bonded modes of water increase. This result suggests that water in bacterial spores is not in a strong hydrogen-bonded state but

rather exists largely as “bound” water that is associated with other spore molecules by weak hydrogen bonding.

Second, the weight of D<sub>2</sub>O in single dormant *B. cereus* spores has been measured as  $4.8 \times 10^{-13}$  g, although there was significant heterogeneity in this value between individual spores in a population. The standard deviation of the measured average weight of D<sub>2</sub>O in single dormant spores was 18% in spore populations, which was much larger than the measurement error (~5%) in the determination of spore water content. This heterogeneity in spore water content may be another example of the heterogeneity in spore populations and might reflect either real differences in the percentages of spores’ wet weight as water or perhaps some other variable such as spore size, which is known to vary significantly in spore populations.<sup>39</sup> However, analysis of Raman spectra of a number of individual D<sub>2</sub>O-loaded spores revealed no relationship between spores’ levels of CaDPA and D<sub>2</sub>O (data not shown). It is certainly possible that the amount of water in an individual spore will affect that spore’s dormancy, germination, and resistance, although to date only effects of spore water content on some spore resistance properties have been documented.<sup>1,2</sup> Perhaps the ability to determine the amounts of water in single spores will provide a technique to probe the effects of water content on other spore properties.

Third, the D<sub>2</sub>O distribution in single dormant bacterial spores has been determined and shows that water distributes unevenly in the spore. This uneven distribution of water in the dormant *B. cereus* spore is consistent with observations of deuterium and hydrogen distribution by nano-SIMS in single *Bacillus thuringiensis* spores in an ultrahigh vacuum.<sup>25</sup> The additional finding in the current study is that the distribution of water, in particular water in the spore core, is very different from that of CaDPA. Indeed, regions of the spore core with the most CaDPA generally had the least water, as CaDPA was concentrated in central regions of the core, while water was concentrated toward the core’s edge. The D<sub>2</sub>O distribution in the spore was also somewhat different from that of protein. The



reason for the uneven distribution of water in the spore core is not known; perhaps water is simply largely excluded from insoluble, and likely primarily crystalline, CaDPA. Certainly, the majority of spore core water is not associated with CaDPA. The spatial resolution of the confocal Raman imaging system used in the current work was diffraction-limited ( $0.46\ \mu\text{m}$  in lateral direction and  $1.2\ \mu\text{m}$  in axial direction), which is relatively large for small *B. cereus* spores ( $\sim 1.5 \times 0.8\ \mu\text{m}$  in size). The confocal analysis of water in the core may be overestimated since some water above and below the core are picked up due to the axial resolution. In fact, the water in the core is estimated to be  $\sim 30\%$  of the total spore water for *B. cereus* spores based on electron microscopy images, and this value is much smaller than the values observed from Figures 3 and 5. Further improvement in the resolution of Raman mapping may provide clearer estimations of the distribution of water and other spore molecules in single spores.

Fourth, the exchange of external  $\text{H}_2\text{O}$  with  $\text{D}_2\text{O}$  in single dormant spores has been measured by Raman microspectroscopy and the exchange rate is extremely fast ( $< 1\ \text{s}$ ). The  $1\ \text{s}$  time resolution of the current Raman measurement system is not fast enough to give detailed information on the kinetics of the water exchange of single spores. However, a time scale of  $1\text{--}2\ \text{s}$  for complete water exchange has been estimated. Hopefully further improvement in the methodology will allow faster measurement times in the future.

Fifth, measurement of  $\text{D}_2\text{O}$  loss from individual  $\text{D}_2\text{O}$ -loaded spores during air-drying has also revealed details of water mobility in spores. It is known that water in the whole spore is "free" in the sense that it can be removed by drying.<sup>13</sup> At the beginning of air-drying,  $\text{D}_2\text{O}$  was lost not only from spore layers outside the core but also from the core itself. After 1 h, all  $\text{D}_2\text{O}$  was lost from outside the core, while the core retained  $\sim 50\%$  of its initial  $\text{D}_2\text{O}$ . This result was directly obtained from the Raman image, consistent with the previous finding that the water content in spore core is  $\sim 30\%$  higher than in the outer structures in an ultrahigh vacuum.<sup>25</sup> Even after 2–3 h, a small amount of  $\text{D}_2\text{O}$  remained at the core's edge. These results are consistent with previous work that found that (1) the mobility of spores' core water is less than that of spore water outside the core<sup>16</sup> and (2) loss of a significant fraction of spore water during drying, most likely core water, is very slow.<sup>14</sup> This difference in the behavior of spore core water and more external spore water can also be seen in the  $\text{D}_2\text{O}$  dehydration curves of single individual spores, as shown in Figure 5 (panels b–e). The slightly faster  $\text{D}_2\text{O}$  loss at the beginning of the drying is the result of the faster release of the outer water, while the subsequent linear  $\text{D}_2\text{O}$  release is the slow release of the core water. Thus, the spores' outer layers retain water poorly, while at certain small areas of the spore core edge, water can be retained for 2–3 h in air at room temperature. The relatively slow removal of spore core water during air drying might be due at least in part to the weak binding of water molecules with other spore components, consistent with the finding that the hydrogen-bonded environment inside the spores has changed to one with a less prominent  $\nu_s(\text{D}-\text{O})$  vibration (Figure 1b). Therefore, the bound water has a slow movement across the spore's inner membrane in air, although they can be exchanged very rapidly by free  $\text{H}_2\text{O}$  molecules upon exposure to liquid  $\text{H}_2\text{O}$ .

In summary, Raman microspectroscopy and Raman imaging appear to provide significant advances in the analysis of the properties and distribution of water in single spore cells.

Indeed, new results applying these techniques to single dormant spores have provided novel information about properties of water in spores and thus new insight into fundamental properties of such spores.

## ■ ASSOCIATED CONTENT

### 📄 Supporting Information

Procedures for Raman acquisition and spectral data processing of single spores and calculation of weights of  $\text{D}_2\text{O}$  in individual spore. This material is available free of charge via the Internet at <http://pubs.acs.org>.

## ■ AUTHOR INFORMATION

### Corresponding Author

\*E-mail: [liy@ecu.edu](mailto:liy@ecu.edu). Tel: 252-328-1858. Fax: 252-328-6314.

### Notes

The authors declare no competing financial interest.

## ■ ACKNOWLEDGMENTS

We are grateful to Dr. Ji Yu for helpful suggestions. This work was supported by a Department of Defense Multidisciplinary University Research Initiative through the U.S. Army Research Laboratory and the U.S. Army Research Office under contract number W911F-09-1-0286 (PS/YQL) and by a grant from the Army Research Office under contract number W911NF-12-1-0325.

## ■ REFERENCES

- (1) Gerhardt, P.; Marquis, R. E. In *Regulation of Prokaryotic Development: Structural and Functional Analysis of Bacterial Sporulation and Germination*; Smith, I., Slepecky, R. A., Setlow, P., Eds.; American Society for Microbiology: Washington, D.C., 1989; pp 43–63.
- (2) Setlow, P. *Curr. Opin. Microbiol.* **2003**, *6*, 550–556.
- (3) Nicholson, W. L.; Munakata, N.; Horneck, G.; Melosh, H. J.; Setlow, P. *Microbiol. Mol. Biol. Rev.* **2000**, *64*, 548–572.
- (4) Setlow, P. *J. Appl. Microbiol.* **2006**, *101*, 514–525.
- (5) Beaman, T. C.; Gerhardt, P. *Appl. Environ. Microbiol.* **1986**, *52*, 1242–1246.
- (6) Black, S. H.; MacDonald, R. E.; Hashimoto, T.; Gerhardt, P. *Nature* **1960**, *185*, 782–783.
- (7) Lewis, J. C.; Snell, N. S.; Burr, H. K. *Science* **1960**, *132*, 544–545.
- (8) Black, S. H.; Gerhardt, P. *J. Bacteriol.* **1962**, *83*, 960–967.
- (9) Neihof, R.; Thompson, J. K.; Deitz, V. R. *Nature* **1967**, *216*, 1304–1306.
- (10) Marshall, B. J.; Murrell, W. G. *J. Appl. Bacteriol.* **1970**, *33*, 103–129.
- (11) Setlow, B.; Setlow, P. *Proc. Natl. Acad. Sci. U.S.A.* **1980**, *77*, 2474–2476.
- (12) Lindsay, J. A.; Beaman, T. C.; Gerhardt, P. *J. Bacteriol.* **1985**, *163*, 735–737.
- (13) Leuschner, R. G. K.; Lillford, P. J. *Microbiology* **2000**, *146*, 49–55.
- (14) Westphal, A. J.; Price, P. B.; Leighton, T. J.; Wheeler, K. E. *Proc. Natl. Acad. Sci. U.S.A.* **2003**, *100*, 3461–3466.
- (15) Plomp, M.; Leighton, T. J.; Wheeler, K. E.; Malkin, A. J. *Biophys. J.* **2005**, *88*, 603–608.
- (16) Sunde, E. P.; Setlow, P.; Hederstedt, L.; Halle, B. *Proc. Natl. Acad. Sci. U.S.A.* **2009**, *106*, 19334–19339.
- (17) Church, B. D.; Halvorson, H. O. *Nature* **1959**, *18*, 124–125.
- (18) Gould, G. W.; Dring, G. J. *Nature* **1975**, *258*, 402–405.
- (19) Setlow, P. *J. Appl. Bacteriol.* **1994**, *76*, 49S–60S.
- (20) Paidhungat, M.; Setlow, B.; Driks, A.; Setlow, P. *J. Bacteriol.* **2000**, *182*, 5505–5512.
- (21) Magge, A.; Granger, A. C.; Wahome, P. G.; Setlow, B.; Vepachedu, V. R.; Loshon, C. A.; Peng, L.; Chen, D.; Li, Y. Q.; Setlow, P. *J. Bacteriol.* **2008**, *190*, 4798–4807.

- (22) Cowan, A. E.; Koppel, D. E.; Setlow, B.; Setlow, P. *Proc. Natl. Acad. Sci. U.S.A.* **2003**, *100*, 4209–4214.
- (23) Maeda, Y.; Fujita, T.; Sugiura, Y.; Koga, S. *J. Gen. Appl. Microbiol.* **1968**, *14*, 217–226.
- (24) Bradbury, J. H.; Foster, J. R.; Hammer, B.; Lindsay, J.; Murrell, W. G. *Biochim. Biophys. Acta* **1981**, *678*, 157–164.
- (25) Ghosal, S.; Leighton, T.; Wheeler, K.; Hutcheon, I. D.; Weber, P. K. *Appl. Environ. Microbiol.* **2010**, *76*, 3275–3282.
- (26) Xie, C.; Mace, J.; Dinno, M. A.; Li, Y. Q.; Tang, W.; Newton, R. J.; Gemperline, P. J. *Anal. Chem.* **2005**, *77*, 4390–4397.
- (27) Chen, D.; Huang, S. S.; Li, Y. Q. *Anal. Chem.* **2006**, *78*, 2936–6941.
- (28) Evanoff, D. D.; Heckel, J.; Caldwell, T. P.; Christensen, K. A.; Chumanov, G. *J. Am. Chem. Soc.* **2006**, *128*, 12618–12619.
- (29) Daniels, J. K.; Caldwell, T. P.; Christensen, K. A.; Chumanov, G. *Anal. Chem.* **2006**, *78*, 1724–1729.
- (30) Kong, L. B.; Zhang, P. F.; Yu, J.; Setlow, P.; Li, Y. Q. *Anal. Chem.* **2010**, *82*, 8717–8724.
- (31) Kong, L. B.; Zhang, P. F.; Yu, J.; Setlow, P.; Li, Y. Q. *Appl. Phys. Lett.* **2011**, *98*, 213703.
- (32) Kong, L. B.; Zhang, P. F.; Wang, G. W.; Yu, J.; Setlow, P.; Li, Y. Q. *Nat. Protoc.* **2011**, *6*, 625–639.
- (33) Kong, L. B.; Setlow, P.; Li, Y. Q. *Analyst* **2012**, *137*, 3683–3689.
- (34) Kong, L. B.; Zhang, P. F.; Setlow, P.; Li, Y. Q. *J. Biomed. Opt.* **2011**, *16*, 120503.
- (35) Nicholson, W. L.; Setlow, P. In *Molecular Biological Methods for Bacillus*; Harwood, C. R., Cutting, S. M., Eds.; John Wiley and Sons: Chichester, U.K., 1990; pp 391–450.
- (36) Walrafen, G. E.; Yang, W.-H.; Chu, Y. C.; Hokmabadi, M. S. *J. Phys. Chem.* **1996**, *100*, 1381–1391.
- (37) Mudalige, A.; Pemberton, J. E. *Vib. Spectrosc.* **2007**, *45*, 27–35.
- (38) McCann, K.; Laane, J. J. *Mol. Struct.* **2008**, *890*, 346–358.
- (39) Huang, S. S.; Chen, D.; Pelczar, P. L.; Vepachedu, V. R.; Setlow, P.; Li, Y. Q. *J. Bacteriol.* **2007**, *189*, 4681–4687.